



ON Semiconductor®

www.onsemi.com

Mains Synchronization for PLC Modems

Introduction

The sensitivity of a communication receiver strongly depends on a correct and reliable synchronization with the transmitter. In power line communication (PLC), the zero crossing of the mains is commonly used for this synchronization. This application note describes the purpose of synchronization and the effects of mismatch (see Problem section); the synchronization used by ON Semiconductor PLC modems (see Synchronization in ON Semiconductor PLC Modems section). Additionally, five zero crossing detection circuits are described and compared (see Zero Crossing Detections Circuits section).

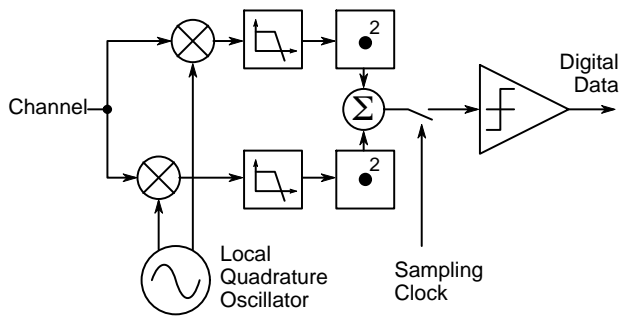


Figure 1. Simple ASK Demodulator

Conclusion

Five zero crossing detector circuits were discussed. The non-isolated detector (see Non-Isolated Circuit section) can be used if no galvanic isolation is required. The conventional topology (see Conventional Detection section) is not suitable to PLC modem applications. The three other circuits (see Low-Voltage Charge Store, Circuit with High-Voltage Charge Storage, and Circuit with Reduced-Length Output Pulse sections) show decreasing power consumption and increasing complexity. Table 2 summarizes measured power consumption at 230 VRMS, component count and a rough cost estimate relative to the conventional solution.

It is critical to compensate the delay introduced by the zero crossing detector which skews the physical bit stream and the bit sampling clock.

In a first step the ZC_ADJUST parameter allows a first adjustment independent of the baud rate in steps of 13 μs.

In a second step the firmware will automatically fine-tune the timing.

APPLICATION NOTE

Problem

Bit Synchronization

Consider the coherent ASK (amplitude shift keying) demodulator of Figure 1. Although a simplification, it illustrates the importance of correct timing.

In Figure 2, waveforms are shown for this demodulator. The original bit stream and the resulting ASK signal (top signals) are put on the channel by the transmitter. For a noise-free channel, the signal after the filter would also be noise-free. In practice, the noise added by the channel is also present after the filter.

When using an optimally aligned sampling clock, the noise and inter-symbol interference (ISI) is tolerable. However, when the receiver samples too late (bottom traces), the detector often misses. Similarly, an early sampling clock will also cause additional bit errors.

The same problem is found in FSK demodulation. Figure 3 shows the digital part of the receiver of the NCN49597 and NCN49599 modems.

When communicating over the power line, a clock signal cannot be sent along with the data. To synchronize the bit sampling clock, the mains zero crossing is commonly used as an alignment point for the transmission clock, and the baud rate is chosen to be a multiple of the mains frequency.

The communication standard will dictate how the transmission clock is linked to the actual mains zero crossing. The PL110 standard (KNX over power line) requires that bits are aligned to the mains zero crossing (without delay); the ON-PL110 firmware provided by ON Semiconductor is compliant with this requirement¹.

¹For completeness' sake we add other standards have different requirement. For instance, the IEC 61334 standard requires a delay of $120 \pm 20 \mu\text{s}$ from the mains zero crossing to the start of the first bit of physical frame. Refer to [1] for details. Please note ON Semiconductor does not provide support the IEC 61334 protocol.

AND9282/D

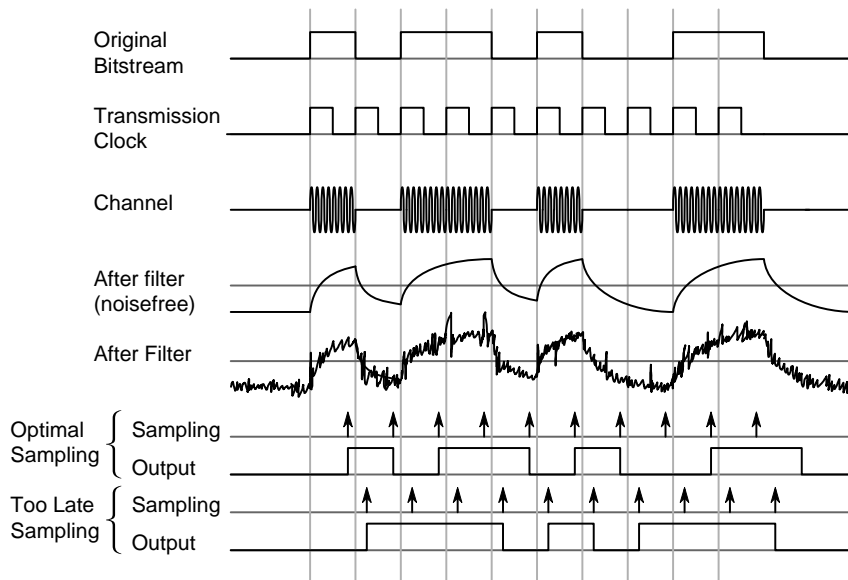


Figure 2. The Coherent Demodulator of Figure 1: Waveforms and the Resulting Data when Sampling Optimally and too Late

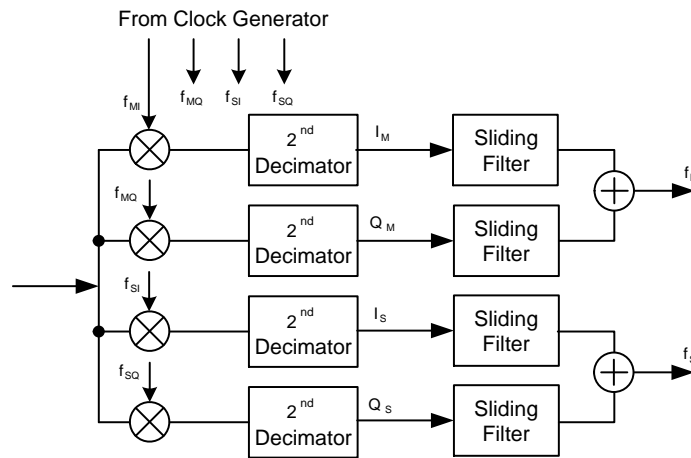


Figure 3. Digital Part of the Receiver of the NCN49597/9

Frame Synchronization

In addition to bit synchronization the receiver also needs to know the start of the physical frame. Obviously, a frame can only start on a physical bit boundary.

The PL110 protocol is indifferent to frame alignment: a frame can start at the start of any bit slot².

Synchronization in ON Semiconductor PLC Modems

Figure 4 shows a block diagram of the synchronization flow in the NCN49597 and NCN49599 PLC modems designed by ON Semiconductor. From the mains, an external zero crossing detector derives a synchronous (50 or

60 Hz) low-voltage clock; it is coupled to the modem through the ZC_IN pin. In the modem a digital PLL constructs the *bit clock* as a multiple of the mains frequency. Additionally the *chip clock* is generated at a rate 8 times faster than the bit clock.

Figure 5 shows the same diagram on a signal level.

²For completeness' sake, we note the IEC standard also requires that a frame starts on the frame clock, a signal with a period of multiple mains periods. The exact period depends on the baud rate, but a frame clock start is always aligned on a mains zero crossing.

AND9282/D

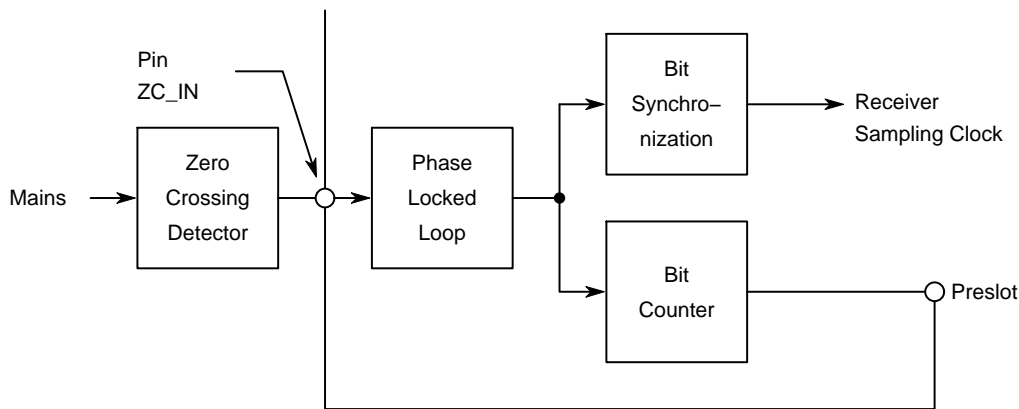


Figure 4. NCN49597 and NCN49599 Bit and Frame Synchronization

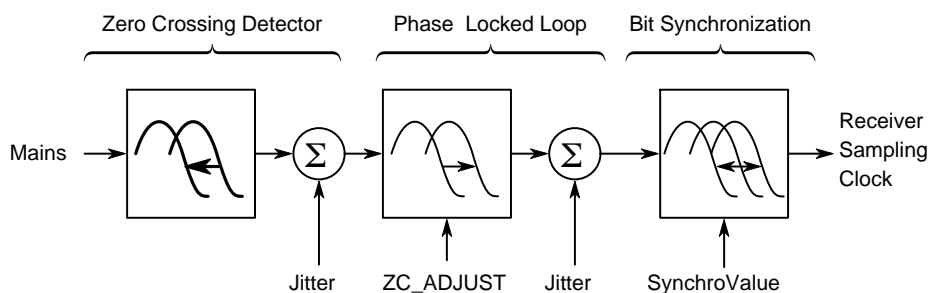


Figure 5. NCN49597/9 Synchronization Signal Diagram. Note the Direction of Delay Arrows

Inevitably, the zero crossing detector suffers from a delay (typically 50–500 ms) and from jitter (typically 2–100 ms).

The phase locked loop can shift the zero crossing signal *forward* (i.e., the inverse of a delay). The amount of this shift is controlled through the ZC_ADJUST register and can be varied between 0 and 3.3 ms. The adjustment period or granularity is 13 μ s. Additionally, jitter of 25 μ s_{pk-pk} is added.

A third time shift is controlled by the SynchroValue setting. This adjustment allows shifting the sampling clock

from –3 to +4 chip clock period in steps of 1 chip period. The transmitter clock is only dependent on the bit clock; SynchroValue only alters the behavior of the receiver. The optimal synchro bit value is deduced automatically by the firmware; no user interaction is required or possible.

Please note that the ON Semiconductor PL110 software solution can use zero crossing information, but does not require it; the software can automatically synchronize to other nodes. This is especially used for communication over DC lines.

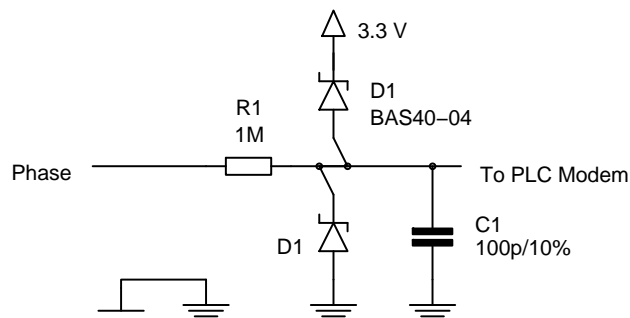


Figure 6. Non-Isolated Zero Crossing Detector

Delay Adjustment

To obtain the desired delay from the mains zero crossing to the bit clock (120 μ s for IDIS, 0 μ s for PL110) the ZC_ADJUST register should be used.

As an example, if a zero crossing detector with a characterized total delay of 95 μ s is used with the ON-PL110 firmware, the best possible ZC_ADJUST value is 7 (7 \times 13 = 91 μ s).

Zero Crossing Detection Circuits

The zero crossing detector generates the mains synchronization signal for the modem. The input is the mains; the output is a 3.3 V TTL signal.

If isolation between modem and mains is not required this circuit can be very simple (see Non-Isolated Circuit section).

Most applications however require galvanic isolation. Optocouplers are an obvious choice, and their conventional application circuit in PLC is described below. However, this

circuit has substantial disadvantages (see Conventional Detection section). In Low-Voltage Charge Store, Circuit with High-Voltage Charge Storage, and Circuit with Reduced-Length Output Pulse sections, we present improved circuits.

In the following, we assume a 230 V mains with variations of -30% and +20%. However, bills of materials for 120 V mains circuits appear in Appendix.

Non-Isolated Circuit

When no galvanic isolation between the mains and the modem is required, a very simple zero crossing circuit can be used (Figure 6).

To protect the ESD protection cell of the modem pin, Schottky diodes reduce the mains voltage to a 0-3.3 V level. A resistor of 1 M Ω limits the current. It is advisable to add a small capacitor to limit the effects of noise and interference.

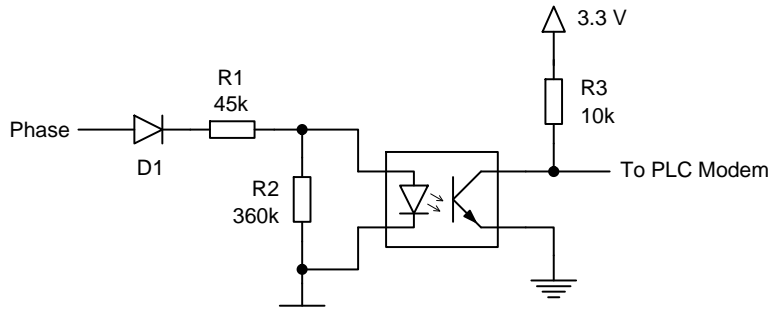


Figure 7. Conventional Isolated ZC Schematic (Variant 1)

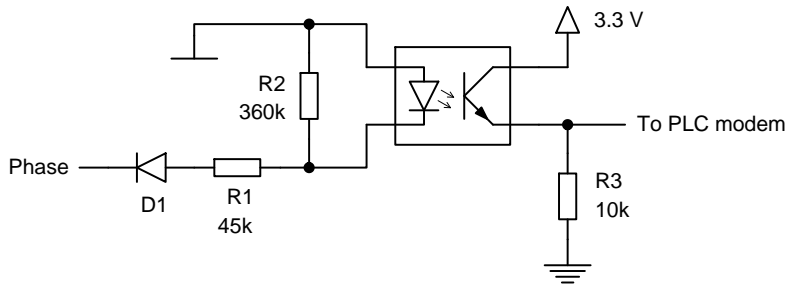


Figure 8. Conventional Isolated ZC Schematic (Variant 2)

Conventional Detection

Two conventional zero crossing detection circuits are shown in Figures 7 and 8.

Diode D1 protects the LED from reverse voltage and reduces dissipation by half. No current flows through the LED at the zero crossing itself, so the detection is significantly delayed. For example, if the peak amplitude of the LED current is set to 5 mA and if the optocoupler needs 0.5 mA to toggle the shift in time would be in the order of 300 μ s. Much bigger currents are drawn after they are no longer needed.

Component Selection

None of the components are critical. It is often convenient to realize the 330 k Ω resistor as a series of smaller resistors. This allows the use of smaller and cheaper packages without exceeding the voltage rating.

The delay introduced by the capacitor can be compensated with the ZC_ADJUST modem setting.

Edge Behavior

The PLL in ON Semiconductor PLC modems synchronizes on the rising edge of the detector output.

The modem can compensate the unavoidable detector delay with an on-chip setting. However, this feature is only effective with constant delay.

Because the rising edge is generated while the LED current is very low the delay is strongly dependent on the current transfer ratio (CTR) of the optocoupler and the $V-I$ curve of the LED. These characteristics vary widely from optocoupler type to type and from sample to sample. They also vary with ageing and temperature.

Most optocouplers have no specification for LED currents below 1 mA at all – especially on the turnoff time and it’s variation over temperature, device and lifetime. This is especially true for the cheaper optocouplers that would be the first choice for volume production of PLC modems.

The rising edge timing also depends on the actual mains voltage. During measurements, a coefficient of $-0.17 \mu\text{s}/\text{V}$ was found (i.e. a higher voltage results in less delay).

It must be noted that the quality and timing of the rising edge is an important difference between the two schematics shown.

In the first variant the rising edge occurs when the optocoupler turns off. Optocoupler turn-off is slower and subjected to larger variations than turn-on. The result is a substantial delay and larger variations of that delay in the field. Additionally, the signal to the PLC modem will occur

prior to the actual zero crossing, since the actual transition comes when the half-wave is almost over and drive current for the LED diminishes. Modems made by ON Semiconductor cannot compensate for this.

The second variant is better in this regard. The rising edge is now influenced by the turn-on characteristics of the photo-transistor, and will occur after the actual zero crossing.

In conclusion, the conventional detector suffers from a large and uncontrollable delay. The second variant circuit is only marginally better than the first.

Component Selection

The breakdown voltage of D_1 must be sufficient while the leakage current must be small; other parameters are not critical.

The combined value of R_1 is calculated for a somewhat arbitrarily chosen peak current under worst case conditions. For a nominal mains voltage of 230 V_{AC} and a desired peak current of 5 mA

$$R_1 = \frac{\sqrt{2} \cdot V_{\text{mains,RMS}}(1 - 30\%) - V_{D1} - V_{LED}}{I_{\text{Peak}}} \quad (\text{eq. 1})$$

$$\approx \frac{228 \text{ V} - 0.6 \text{ V} - 3 \text{ V}}{5 \text{ mA}} = 45 \text{ k}\Omega$$

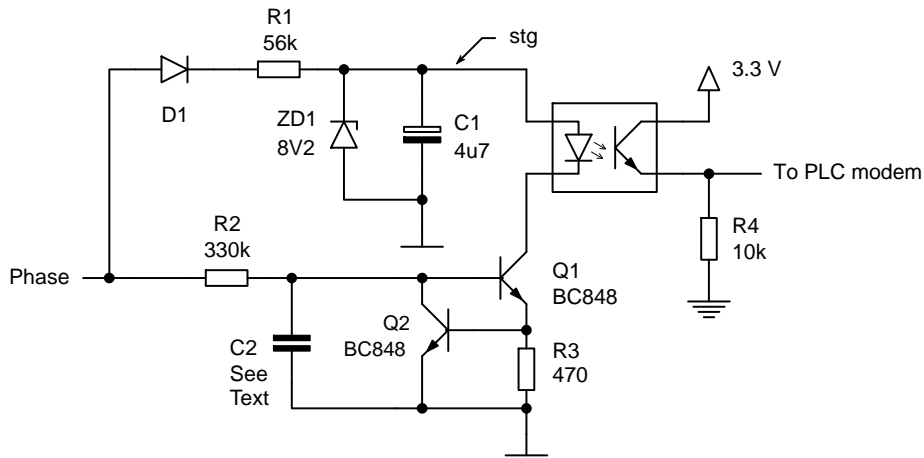


Figure 9. Improved Isolated ZC Schematic

The calculation of the power dissipation must take the highest possible mains voltage into account. This results in:

$$P = 50\% \cdot \frac{(V_{\text{Mains}} \cdot 120\%)^2}{R_1} = 850 \text{ mW} \quad (\text{eq. 2})$$

The dissipation rating of R_1 and cooling arrangements must ensure reliable operation over the full operating temperature range.

R_1 also has to withstand the maximum voltage on the power line; often a series connection of SMD resistors is advantageous to maintain the benefits of surface mounting while meeting the maximum voltage requirements.

R_2 is required to avoid breakdown of the optocoupler LED. It is sized to ensure the current through R_2 is negligible.

Low-Voltage Charge Storage

An improved ZC circuit can be used to ensure more reliable operation without excessive dissipation or high-end optocouplers (Figure 9).

D_1 , R_1 , C_1 and ZD_1 form a simple power supply. The charge on C_1 allows current for operating the LED to be drawn at the time of zero crossing, when the conventional solution has negligible current drive capabilities at that time.

Two NPN transistors, Q_1 and Q_2 form a constant current sink. Local negative feedback yields a constant voltage over R_3 (this is the base-emitter voltage of Q_2 , some 650 mV at the design operating point), and as consequence a constant current through R_3 .

If the current gain of both transistors is high enough this is about equal to the collector current of Q_1 and the LED current.

The power line turns on the CCS during the positive half-wave, when the current through R_2 is sufficient to power up the base of Q_1 . During the negative half wave the Q_1 base voltage is forced to about -0.65 V as the base-collector junction of Q_2 is forward biased, clamping the mains voltage.

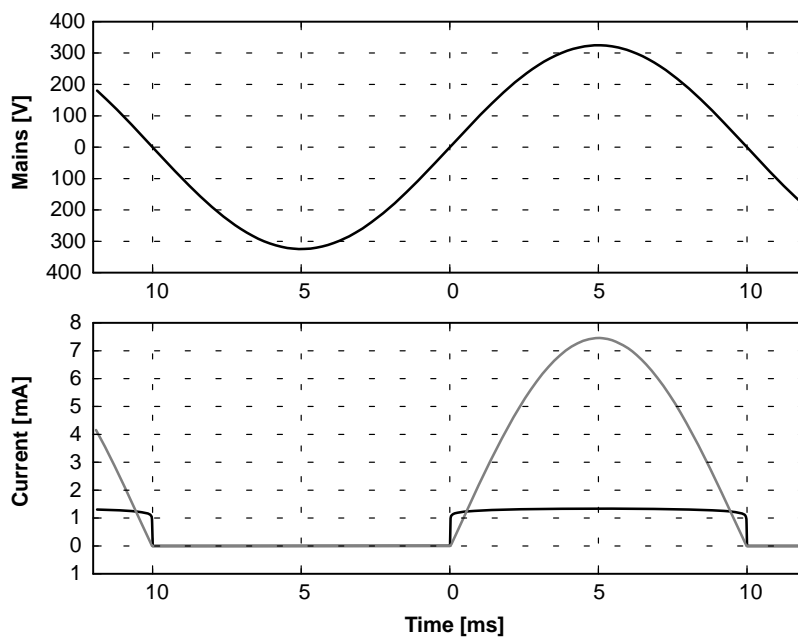


Figure 10. Current Waveforms through the LED for the Conventional (Grey) and the Improved Detector (Black).

Figure 10 shows the simulated currents for the conventional (grey trace) and the improved (black) ZC circuits. The LED drive current for the improved circuit is much close to an ideal square wave, which significantly narrows the uncertainty window in which the zero crossing will be detected.

In the conventional circuit the current is much smaller close to the real zero crossing – $160 \mu\text{A}$ at $300 \mu\text{s}$ after the actual zero crossing. With the improved ZC circuit 1 mA is reached in $40 \mu\text{s}$, and this delay can be further shortened with some reduction of R_2 .

The measured delay between the actual power line zero crossing and the isolated side of 6 HCPL–817 optocouplers,

in both the conventional and the improved circuits, is represented in Table 1.

The total device-to-device variation is reduced from $93 \mu\text{s}$ to $24 \mu\text{s}$. An even bigger effect is expected with optocouplers with worse CTR at low LED currents.

Additionally, measurements on TCET–1109, SFH615A–3 and NEC 2501 optocouplers show a type-to-type variation of only $10 \mu\text{s}$.

It is important to note that these measurements are done at room temperature and without any ageing. Drive techniques used in the improved ZC circuit will also reduce further variations in the field.

Table 1. MEASURED DELAY OF THE CONVENTIONAL AND THE IMPROVED ZERO CROSSING DETECTOR (6 HCPL–817 Optocoupler Samples)

Sample	Conventional Circuit	Improved Circuit
1	374 μs	70 μs
2	281 μs	52 μs
3	298 μs	46 μs
4	298 μs	61 μs
5	298 μs	62 μs
6	290 μs	55 μs

Component Selection

The reverse polarity protection diode D_1 must withstand the peak reverse voltage expected on the mains. Besides from leakage (which should be below $100\ \mu\text{A}$ in the full operating temperature range) there are no special requirements for this diode.

The LED drive current in the suggested schematics is around $1.3\ \text{mA}$, and is defined by the $650\ \text{mV}$ voltage drop over the $470\ \Omega$ value of R_3 . Increasing this current is certainly possible, but will also require proportional change in other components since all the currents will proportionally scale.

The value of the reservoir capacitor C_1 suggested in Figure 2 ($4.7\ \mu\text{F}$) is a good compromise between voltage ripple and start-up time. The available charge current is limited by the power dissipation in R_1 and the need to keep the efficiency high. Values shown in Figure 2 give a start-up time of $50\ \text{ms}$ for proper zero cross detection and $250\ \text{ms}$ until C_1 is fully charged.

The voltage ripple is below $500\ \text{mV}$, which is no problem for the CCS performance. The current ripple through C_1 is small (below $1\ \text{mA}$) so part selection is straightforward. The rated voltage must exceed the $8.2\ \text{V}$ zener voltage.

The choice of R_1 is directed by the average current balance. If R_1 is too low excess power is dissipated in the zener diode. If R_1 is too high, LED current will be limited by R_1 and not by the current source; the circuit will behave identical to the conventional solution.

The current drawn over the positive half-wave dominates. Over this period a constant current of $1.3\ \text{mA}$ is drawn by the LED. To ensure the voltage is well stabilized by the zener diode about as much current must flow through the zener. Over the same period the average current through R_1 can be approximated as the RMS voltage of the mains divided by R_1 .

It follows the latter current must be sufficiently higher than the load currents under worst case conditions, which comprises:

- Lowest mains voltage anticipated; in our case $230\ \text{V}_{\text{RMS}} \cdot 30\%$
- Highest LED current:
 - ◆ The $650\ \text{mV}$ V_{BE} typical for room temperature would grow to $800\ \text{mV}$ at -55°C
 - ◆ The lowest R_3 value foreseen: as an example, 5% resistance tolerance

Together this would result in $1.8\ \text{mA}$ (a 30% increase).

For this design example this would result in $63\ \text{k}\Omega$. We select an E12 value of $56\ \text{k}\Omega$. Once the value has been chosen the worst-case power dissipation can be calculated. Again, we approximate the current through R_1 as the RMS mains voltage (now the highest possible) divided by the worst-case R_1 during half of the time. This results in $(230\ \text{V}_{\text{RMS}} + 20\%)^2 / (56\ \text{k}\Omega \cdot 5\% \text{ tolerance}) / 2 = 715\ \text{mW}$.

Again, depending on cost considerations R_1 may be split in series-connected lower value resistors.

R_2 can be reduced 2 to 3 times if further improvement of the delay is desired at the expense of additional power dissipation. However, a constant delay is more important than a small delay.

Q_1 and Q_2 operate at $V_{\text{CE}} < 10\ \text{V}$ and $I_{\text{C}} \approx 1\ \text{mA}$. High current gain is desired. The BC848 shown in Figure 9 is a reasonable choice; a large number of alternatives is available.

The value of R_4 is a compromise. Low values result in lower delay times while higher values ensure less circuit sensitivity to the CTR of the optocoupler. $10\ \text{k}\Omega$ will be reasonable in most designs. It is always a good idea, though, to check a couple of values (e.g. $3.3\ \text{k}\Omega$ and $33\ \text{k}\Omega$) prior to volume production start. A full voltage swing at the ZC pin is advisable for reliable operation. If the voltage swing is below $3.3\ \text{V}$ the designer must verify that the CTR of the selected optocoupler is sufficient at the designed current.

For the design example discussed above a CTR of 100% would give $1.3\ \text{mA}$ in the photo-transistor, which should be more than sufficient to get the full voltage swing on the ZC pin.

In case optocouplers with significantly different CTR (Current Transfer Ratio) for low LED forward currents have to be used the values of R_1 , R_2 and R_3 may have to be scaled (down) accordingly. For example, if a drive current of $2.5\ \text{mA}$ is found to be sufficient with another series of optocouplers their values would need to be decreased two times. This would inevitably increase power drained from the mains and higher component cost and is most likely never desired, which limits the choice of optocouplers.

However, the demands towards optocouplers are even higher in the conventional schematic; therefore the improved ZC schematic is advantageous also when cost reduction is targeted with lower grade optocouplers.

The optocoupler remains the key in isolated ZC designs. However, finding low-cost devices with even not low but at all specified turn-on times at $1\ \text{mA}$ drive currents over temperature and lifetime is often a problem. As a general rule devices specified with highest CTR at lowest LED forward current would be significantly better. The improved design relaxes the optocoupler requirements since the trigger point is made less sensitive to characteristics variations.

Compared to the design example above for the conventional detector, the dissipation is not much lower, but the timing is now reliable. The component cost has only increased marginally.

Circuit with High-Voltage Charge Storage

If a further reduction of power consumption is required the circuit depicted in Figure 11 can be employed. The basic operating principle remains the same; however, the regulated voltage is now derived directly from the mains and is thus much higher (about $300\ \text{V}_{\text{DC}}$ instead of $8.2\ \text{V}_{\text{DC}}$).

Additionally, the base resistor R_2 of Figure 9 has been replaced by a diode-resistor combination, halving the power dissipated in R_2 . To ensure the base voltage of Q_1 is

well-controlled during the negative half-cycle, R₃ has been added.

The power consumption is now halved compared to the circuit of Figure 9 at somewhat higher cost. For a full comparison refer to the Appendix.

Measured waveforms are shown in Figure 12 (solid black). The upper pane shows the mains input and the top plate voltage of C₁; below the output signal is shown. The third pane shows the currents³ through the optocoupler diode (rectangular wave current) and the total current flowing into the circuit.

Three simulated waveforms are also shown (dashed grey lines): the C₁ top plate voltage and both currents.

The difference between the simulated and measured LED current is small, but this leads to a more pronounced difference in the most critical parameter: the lowest voltage on C₁. This once again underlines the importance of carefully verifying circuit behavior.

³After capture, both signals were low-pass filtered with a bandwidth of 30 kHz to reduce displayed noise. It was verified this filtering does not hide significant signal features.

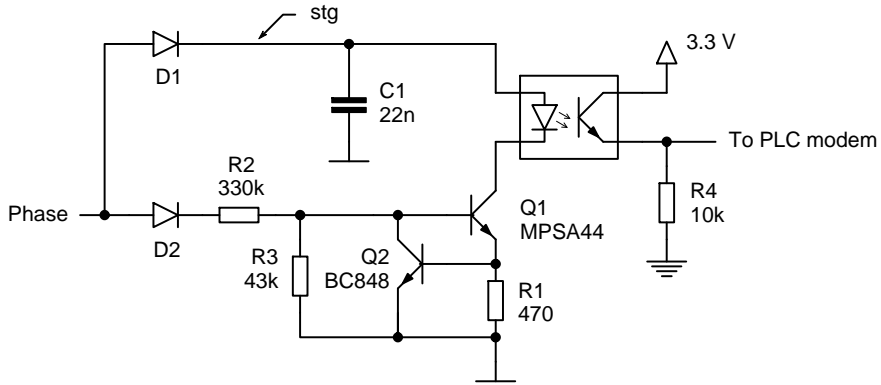


Figure 11. Schematic of the Detector with High-Voltage Charge Storage

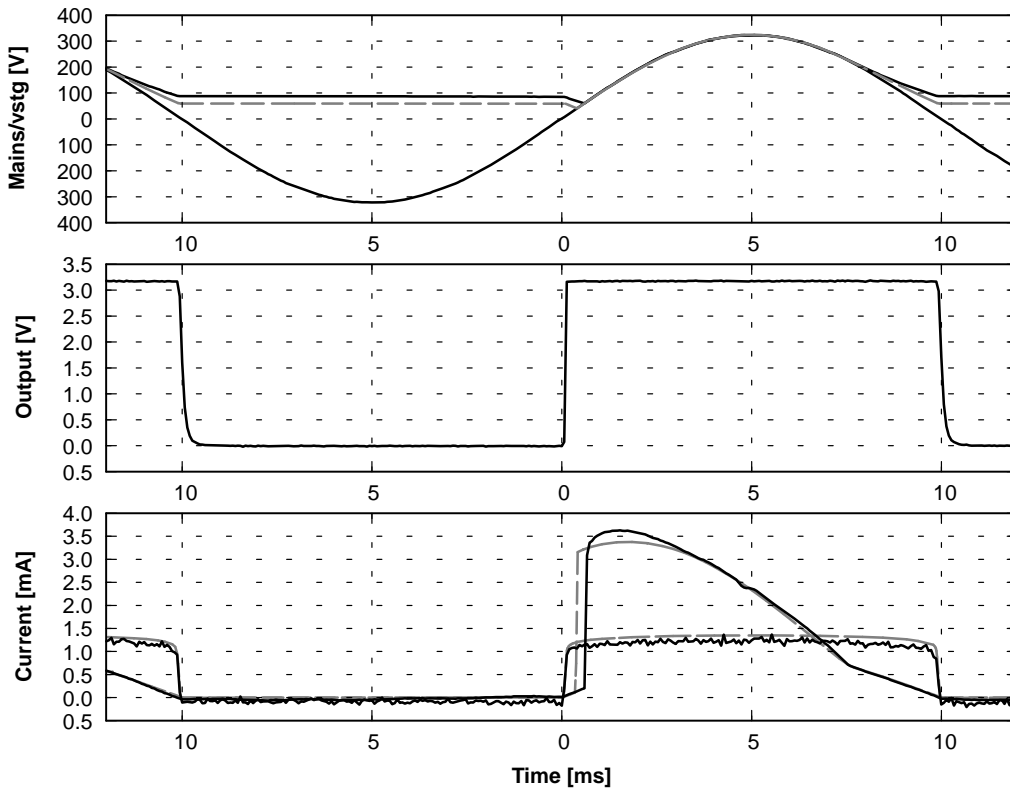


Figure 12. Measured (Solid Black) and Simulated Signals for the High-Voltage Charge Storage Pulse Detector
(Refer to the text for details)

Component Selection

First chose the minimal allowable voltage on C_1 , $VC_{1,min}$. The current source requires some voltage drop to function properly. The drop across the LED must be added to this. $VC_{1,min} = 10\text{ V}$ is a safe starting point; a lower value does not result in a substantial cost gain.

C_1 is recharged during the rising half of the positive mains period. The charge on C_1 is used from $t = t_{start}$, when

$$\frac{d}{dt} V_{Mains}(t) \Big|_{t = t_{Start}} = \frac{I_{LED}}{C_1} \quad (\text{eq. 3})$$

which leads immediately to

$$\sqrt{2} \cdot V_{Mains} \cdot 2\pi \cdot f_{Mains} \cdot \cos(2\pi \cdot f_{Mains} \cdot t_{Start}) = \frac{I_{LED}}{C_1} \quad (\text{eq. 4})$$

At the falling zero crossing, the current source switches off. The charge is again used from the rising zero crossing until the mains voltage rises to $V_{C1}(t) + V_D$. By design requirement, at this point $V_{C1}(t = t_{min}) = VC_{1,min}$. It may be seen that

$$t_{min} = \frac{1}{2\pi \cdot f_{Mains}} \arcsin \frac{V_{C1,min}}{\sqrt{2} \cdot V_{Mains,RMS}} \quad (\text{eq. 5})$$

The worst-case condition is a low mains voltage. As an example, if a 30% drop below nominal is foreseen,

$$C_1 > I_{LED} \cdot \frac{\frac{1}{2} \cdot t_{Mains} - t_{Start} + t_{min}}{\sqrt{2} \min V_{Mains,RMS} - V_{Q1,min}} \quad (\text{eq. 6})$$

$$= \frac{V_T}{R_1} \cdot \frac{\frac{1}{2} \cdot t_{Mains} - t_{Start} + t_{min}}{\text{nom } V_{Mains,RMS}(1 - 30\%) - V_{Q1,min}}$$

As the right hand side of Equation 6 depends on C_1 , an analytical expression for C_1 is not readily deduced, but a numerical value of 18 nF can be calculated for the conditions given. Simulation confirms this.

The only requirements for the diodes are sufficient breakdown voltage and low leakage current. The peak voltage rating of D_2 should allow for the highest mains peak voltage expected. The peak voltage rating of D_1 should exceed *twice* the mains peak voltage; the voltage over C_1 doubles the voltage over D_1 during the negative mains alternation.

C_1 and Q_1 must be high-voltage types. An MPSA44 transistor (suggested for Q_1) has a collector-emitter breakdown voltage of 400-V. Q_2 can be a low-voltage transistor; BC848 is suggested. R_1 can be designed as before, keeping in mind that C_1 must scale with the desired LED current (Equations 4 and 6).

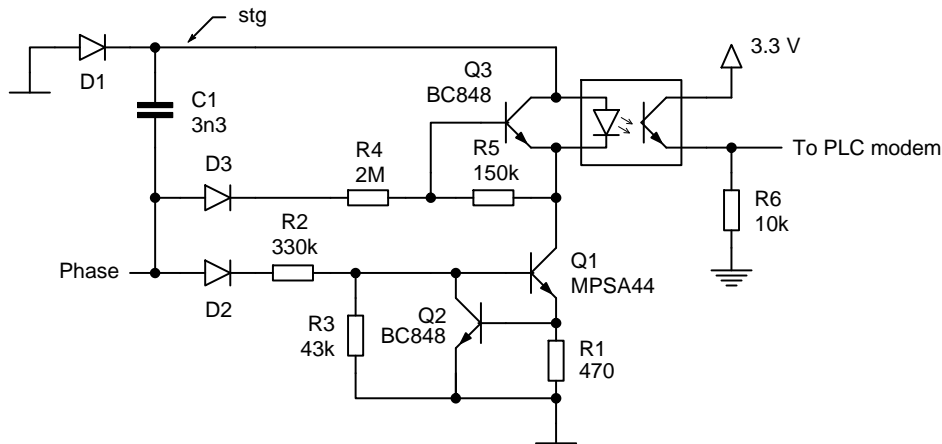


Figure 13. Schematic of the Detector with Reduced Output Pulse Length

Circuit with Reduced-Length Output Pulse

Even lower power consumption can be obtained at the cost of a more complex circuit (Figure 11).

During the first half of the negative half-cycle, C_1 is charged through D_1 . During the second half, D_1 no longer conducts and the voltage on the top plate of C_1 (the net denoted ‘stg’ in Figure 13) rises together with the mains voltage.

Slightly after the zero crossing, the current source (Q_1 , Q_2 , &c.) switches on and the charge on C_1 is consumed. Therefore, the LED will not conduct during the full positive half-cycle. The exact conduction time will depend on the charge on C_1 . Thus, the average LED current consumption can be reduced to a very low value.

In contrast to the circuits discussed before the output pulse duty cycle is now substantially less than 50%. However, as all ON Semiconductor modems synchronize on the rising edge of the zero crossing detector output, correct alignment is maintained.

While the rising edge is well defined by the turn-on of the current source, the falling edge is significantly less controlled if the output duty cycle is less than 25%. In this operating mode, the mains voltage continues to rise even after the charge on C_1 has been depleted. This results in an low but ill-defined current through the optocoupler LED; in turn, this results in an ill-defined falling edge.

Although correct operation can be maintained by buffering the output with a logic gate, the solution depicted

in Figure 13 is more robust. After the voltage on *stg* falls below the mains voltage, Q_3 bypasses the optocoupler LED entirely, resulting in a clean falling edge.

Some measured waveforms are shown in Figure 14 and the top place voltage of C_1 ; below the output signal is shown.

The third pane shows the currents⁴ through the optocoupler diode (rectangular wave current) and the total current consumption of the circuit. Three simulated waveforms are also shown (dashed grey lines): the C_1 top plate voltage and both currents.

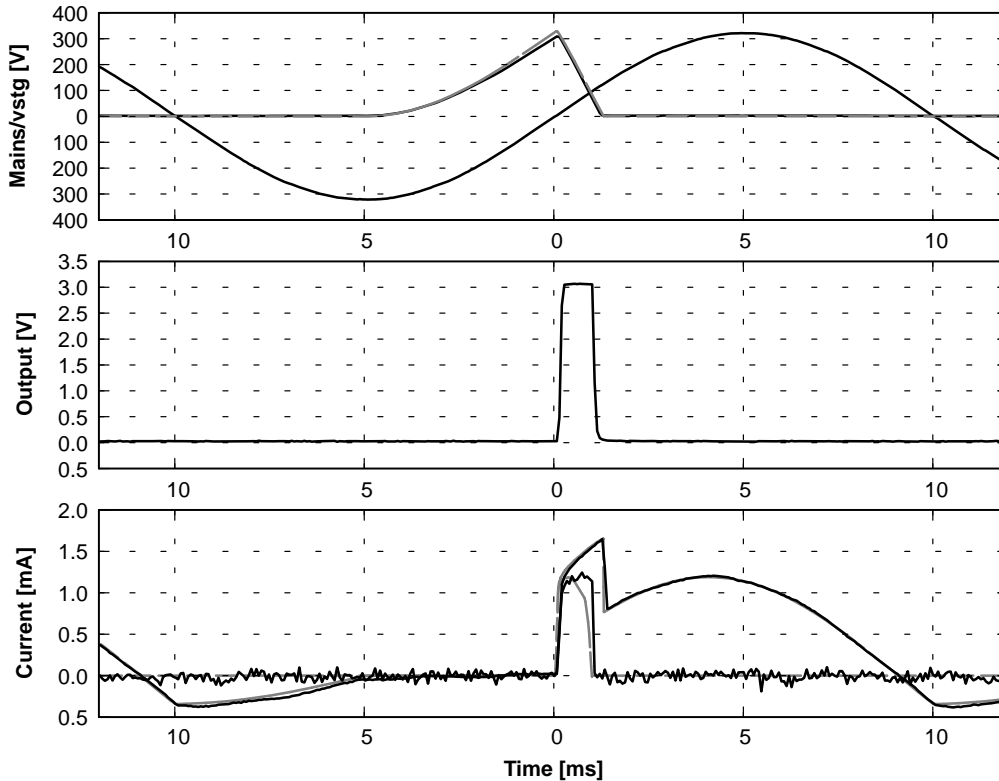


Figure 14. Measured (Solid Black) and Simulated Signals for the Reduced-Length Output Pulse Detector
(Refer to the text for details)

Compared to the circuit of Figure 11, the power consumption is halved again, with the component cost somewhat higher. For a full comparison refer to the conclusion (see Appendix).

The value can be easily calculated if the pulse time is short. Under this condition, a first-order approximation of the mains voltage around the zero-crossing can be employed. The voltage V_C over the capacitor diminishes as current is drawn. The voltage on the net *stg* is then given by (with $t = 0$ at the positive zero crossing)

$$V_{stg}(t) = V_{Mains}(t) + V_C(t) \quad (\text{eq. 7})$$

$$\approx t \left. \frac{dV_{Mains}(t)}{dt} \right|_{t=0} + \left(V_C(t=0) - \frac{t \cdot I_{LED}}{C_1} \right)$$

When the capacitor charge has been exhausted $V_{stg}(t) \approx 0$; by solving for t one can determine the value of C_1 for a given LED current, mains voltage and pulse time t . The actual pulse will be somewhat shorter due to Q_3 . The 3.3 nF value given maintains an 800 ms pulse even if the mains voltage is 30% below nominal.

The diodes C_1 and Q_1 must be high-voltage types. Both Q_2 and Q_3 can be low-voltage transistors. R_1 can be changed as

before, keeping in mind that C_1 must scale with the desired LED current.

The power dissipation of the components should not be problematic, but the voltage rating of R_2 and R_4 must be sufficient to withstand the mains voltage.

Component Selection

Again, the value of C_1 must allow for reliable operation under worst-case conditions; that is, under low mains voltage.

All diodes should have a peak voltage rating exceeding the highest expected mains peak voltage.

Safety

Safety must be considered carefully for measurements. A current as low as 30 mA through the heart can be lethal. Recommendations for safer measurements on circuit with deadly voltages such as zero crossing detectors are beyond the scope of this document; they can be found in [2] and [3, section Safety].

⁴As in Figure 12, the currents are band-limited to 30 kHz.

Table 2. ZERO CROSSING CIRCUITS COMPARED

(Measurement power consumption, component count and cost relative to the conventional solution.)

Circuit	Components	230 V _{AC} Variant		120 V _{AC} Variant	Figure
		Cost	Dissipation	Dissipation	
Non-Isolated	3	0.2	50 mW	30 mW	6
Conventional	5	1.0	590 mW	290 mW	7
Low-Voltage Charge Storage	10	1.5	610 mW	400 mW	9
High-Voltage Charge Storage	10	1.9	230 mW	120 mW	11
Reduced-Length Output Pulse	15	2.3	110 mW	50 mW	13

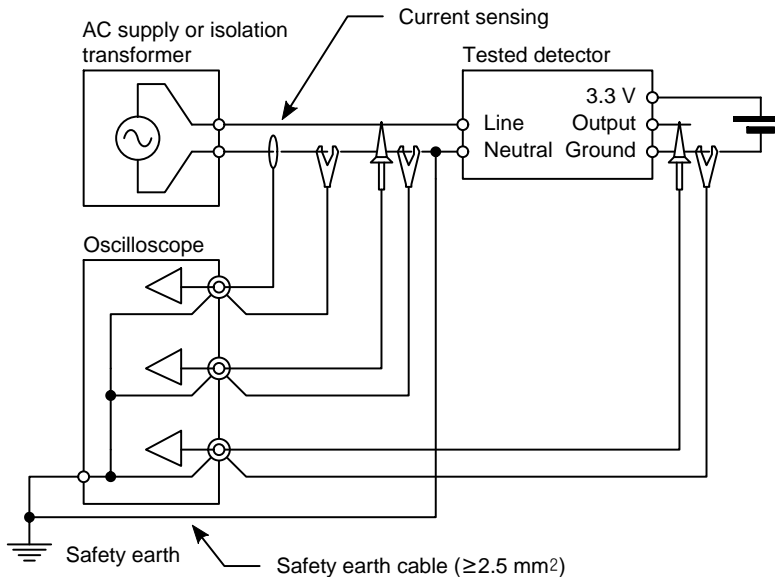


Figure 15. Measuring the Power Consumption, Delay and Jitter of a Zero Crossing Detector

Evaluating Circuits

Already noted several times in the preceding sections, it can not be stressed enough the designed circuit must be tested thoroughly. The substantial variation in available optocoupler types will require a complete evaluation over temperature and mains voltage. Part-to-part variations must also be considered carefully.

Fortunately, testing a zero crossing detector is fairly simple. An adjustable AC source (either an AC laboratory supply or an autotransformer) must be available to verify correct operating within the design voltage range.

To measure the current, a current probe may also be used provided it is sufficiently sensitive.

Alternatively, use a small series resistor (about 100 Ω) in the neutral line and acquire the signal across it with an oscilloscope. A high-voltage differential probe is the safest measurement method (Figure 16, right) but a generic probe can be used if care is taken to ensure safety (Figure 16, left).

Noise can be especially problematic with switch-mode AC sources. The current, and therefore the voltage across the resistor, is small. If noise and tones interfere with the measurement, a filter may be used. The filters shown in Figure 16 have a 3 dB bandwidth exceeding 10 kHz.

The consumed power is derived from the current waveform by integrating with the measured mains voltage waveform⁵. Low-pass filtering the acquired oscilloscope data can improve the accuracy of the measured power consumption value. Software such as Numerical Python, Matlab or Octave are useful for this.

Jitter may be estimated by triggering the oscilloscope on the true mains zero crossing and configuring the display to show persistent traces⁶. As an example, the screen image of Figure 17 shows the mains (left trace) and the detector output. A jitter of approximately 6.8 μs is found with the oscilloscope cursors. The average delay is about 93 μs.

Alternatively, a script can repeatedly measure the delay. This approach has the advantage that statistical data becomes available.

⁵Multiplying the current with the RMS voltage of course overestimates the dissipation as it includes reactive power. This power is especially significant for the reduced-length output pulse circuit.

Care must be taken to deskew the current and voltage measurements. Skew between both is especially significant when using a split-core current probe.

⁶Tektronix, who introduced this feature, calls this “digital phosphor”.

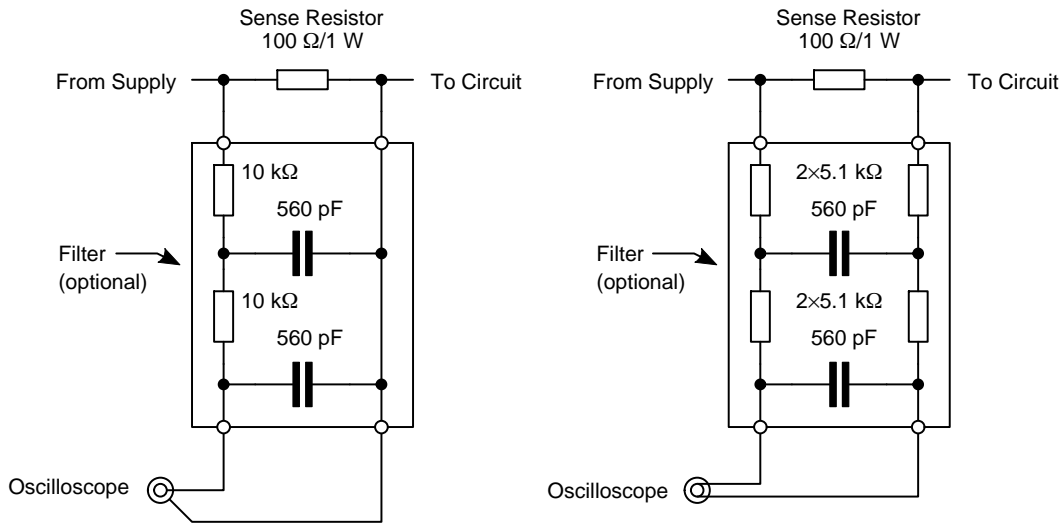


Figure 16. Measuring the Current with a Single-Ended (Left) or Differential Oscilloscope Probe (Detail of Figure 15)

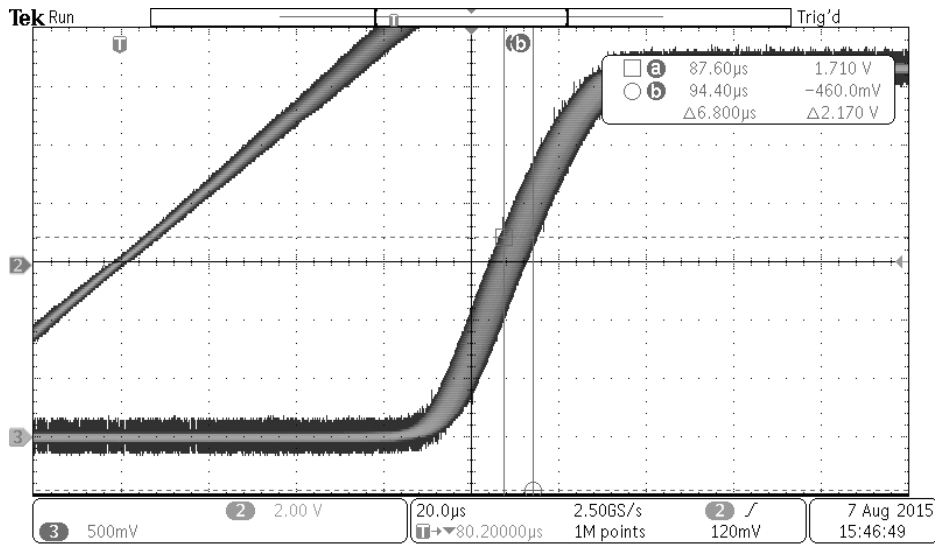


Figure 17. Measuring the Output Jitter Current with an Oscilloscope Configured to Show Persistent Traces. Mains (Left) and Detector Output are Shown

Volume Production

Optocoupler characteristics can vary from batch to batch, especially at low drive currents.

Therefore, we recommend to measure the delay as part of outgoing testing in volume production.

Summary

Table 2 compares the power dissipation of the zero crossing detector circuits discussed above. For the 230 V_{AC} variant, a cost estimate relative to the conventional solution is also given.

APPENDIX

Component Lists

The following bills of materials are given as an example only. In practice, the choice of optocoupler will drive the design.

The optocoupler and its pull-up resistor are not included.

Non-Isolated Detection

Table 3. NON-ISOLATED DETECTION

Component	230 V _{AC} Variant	120 V _{AC} Variant
C1	100 pF	150 pF
D1	BAS40-04	BAS40-04
R1	1 MΩ	510 kΩ

Conventional Detection

Values are given for a 5 mA peak current; this choice must be verified for the selected optocoupler.

Table 4. CONVENTIONAL DETECTION

Component	230 V _{AC} Variant	120 V _{AC} Variant
D1	S1FLJ	BAS21LT1G
R1	43 kΩ	24 kΩ
R2	300 kΩ	300 kΩ
R3	10 kΩ	10 kΩ

Low-Voltage Charge Storage

Values are given for a 1.3 mA peak current; this choice must be verified for the selected optocoupler. It might be convenient to replace the BC848 transistors by a dual transistor such as the NTJD4401NT2G.

Table 5. LOW-VOLTAGE CHARGE STORAGE

Component	230 V _{AC} Variant	120 V _{AC} Variant
C1	4.7 μF/16 V	4.7 μF/16 V
C2	See Text	See Text
D1	S1FLJ	BAS21LT1G
Q1, Q2	BC848BWT1G	BC848BWT1G
R1	56 kΩ	22 kΩ
R2	330 kΩ	160 kΩ
R3	470 Ω	470 Ω
R4	10 kΩ	10 kΩ
ZD1	MM3Z8V2ST1G	MM3Z8V2ST1G

High-Voltage Charge Storage

Table 6. HIGH-VOLTAGE CHARGE STORAGE

Component	230 V _{AC} Variant	120 V _{AC} Variant
C1	22 nF/450 V	33 nF/450 V
D1	S1FLK	S1FLJ
D2	S1FLJ	BAS21LT1G
Q1	MPSA44	MMBTA42LT1G
Q2	BC848BWT1G	BC848BWT1G
R1	470 Ω	470 Ω
R2	330 kΩ	160 kΩ
R3	43 kΩ	43 kΩ
R4	10 kΩ	10 kΩ


Reduced-Length Output Pulse

Table 7. REDUCED-LENGTH OUTPUT PULSE

Component	230 V _{AC} Variant	120 V _{AC} Variant
C1	3.3 nF/450 V	6.8 nF/250 V
D1, D2, D3	S1FLK	BAS21LT1G
Q1	MPSA44	MMBTA42LT1G
Q2, Q3	BC848BWT1G	BC848BWT1G
R1	470 Ω	470 Ω
R2	330 kΩ	160 kΩ
R3	43 kΩ	43 kΩ
R4	2 MΩ	2 MΩ
R5	150 kΩ	150 kΩ
R6	10 kΩ	10 kΩ

REFERENCES

- [1] IEC. Automatisation de la distribution à par l'aide de systèmes de communication à courants porteurs – partie 4: Protocoles de communication de données – Section 32: Couche liaison de données – Contrôle de liaison logique (LLC), September 1996.
- [2] Tektronix. Fundamentals of floating measurements and isolated input oscilloscopes, February 2005. Application note, online at <http://info.tek.com/www-fundamentalsof-floating-measurements-andisolated-input-oscilliscopes.html>
- [3] Pierre Woestyn, Peter Cox, et al. *Evaluation kit for power-line communication user manual*. ON Semiconductor, July 2015.

ON Semiconductor and  are trademarks of Semiconductor Components Industries, LLC dba ON Semiconductor or its subsidiaries in the United States and/or other countries. ON Semiconductor owns the rights to a number of patents, trademarks, copyrights, trade secrets, and other intellectual property. A listing of ON Semiconductor's product/patent coverage may be accessed at www.onsemi.com/site/pdf/Patent-Marking.pdf. ON Semiconductor reserves the right to make changes without further notice to any products herein. ON Semiconductor makes no warranty, representation or guarantee regarding the suitability of its products for any particular purpose, nor does ON Semiconductor assume any liability arising out of the application or use of any product or circuit, and specifically disclaims any and all liability, including without limitation special, consequential or incidental damages. Buyer is responsible for its products and applications using ON Semiconductor products, including compliance with all laws, regulations and safety requirements or standards, regardless of any support or applications information provided by ON Semiconductor. "Typical" parameters which may be provided in ON Semiconductor data sheets and/or specifications can and do vary in different applications and actual performance may vary over time. All operating parameters, including "Typicals" must be validated for each customer application by customer's technical experts. ON Semiconductor does not convey any license under its patent rights nor the rights of others. ON Semiconductor products are not designed, intended, or authorized for use as a critical component in life support systems or any FDA Class 3 medical devices or medical devices with a same or similar classification in a foreign jurisdiction or any devices intended for implantation in the human body. Should Buyer purchase or use ON Semiconductor products for any such unintended or unauthorized application, Buyer shall indemnify and hold ON Semiconductor and its officers, employees, subsidiaries, affiliates, and distributors harmless against all claims, costs, damages, and expenses, and reasonable attorney fees arising out of, directly or indirectly, any claim of personal injury or death associated with such unintended or unauthorized use, even if such claim alleges that ON Semiconductor was negligent regarding the design or manufacture of the part. ON Semiconductor is an Equal Opportunity/Affirmative Action Employer. This literature is subject to all applicable copyright laws and is not for resale in any manner.

PUBLICATION ORDERING INFORMATION

LITERATURE FULFILLMENT:

Literature Distribution Center for ON Semiconductor
19521 E. 32nd Pkwy, Aurora, Colorado 80011 USA
Phone: 303-675-2175 or 800-344-3860 Toll Free USA/Canada
Fax: 303-675-2176 or 800-344-3867 Toll Free USA/Canada
Email: orderlit@onsemi.com

N. American Technical Support: 800-282-9855 Toll Free
USA/Canada
Europe, Middle East and Africa Technical Support:
Phone: 421 33 790 2910
Japan Customer Focus Center
Phone: 81-3-5817-1050

ON Semiconductor Website: www.onsemi.com

Order Literature: <http://www.onsemi.com/orderlit>

For additional information, please contact your local Sales Representative